

1
2
3
4
5
6
7
8
9
10
11
12
13
14
15
16

An Economical Open-Source Lagrangian Drifter Design to Measure Deep Currents in Lakes

Lewis McCaffrey¹ and Alexander L. Koeberle²

¹New York State Department of Environmental Conservation, Syracuse, New York, USA.

²Department of Natural Resources and the Environment, Fernow Hall, Cornell University, Ithaca, New York, USA, 14853.

Corresponding author: Lewis McCaffrey (lewis.mccaffrey@dec.ny.gov)

Key Points:

- An economical, open-source Lagrangian drifter designed to collect current data on lakes <200km² was evaluated against existing designs.
- The new design was tested in deep inland lakes in the Finger Lakes region of New York, USA and is effective at tracking deep currents.
- The ease and low-cost of fabrication and launch/recovery should facilitate use of this design by less-advantaged communities & researchers.

17 **Abstract**

18 The objective was to construct and test an economical, accurate, and open-source Lagrangian
19 drifter design suitable for lakes $<200 \text{ km}^2$. Lagrangian drifters are used to trace water currents in
20 marine and freshwater settings and comprise of a low-friction surface float containing
21 instrumentation for location and environmental measurement, tethered to a high-friction drogue
22 at the depth of interest. Oceanic drifters are robust but expensive, and this design tailored to
23 inland lake waterbodies fills a durability and cost gap for lake environments. Water-following
24 characteristics were tested using theoretical drag coefficient calculations, practical drag
25 measurements, and comparison of wind and drifter vectors while deployed on two deep inland
26 lakes (maximum area 175 km^2) in the Finger Lakes region of New York, USA. The ratio of drag
27 between float and drogue met or exceeded the minimum value of 40 recommended in the
28 literature, and the vectors of wind and drifter during deployment were independent of one
29 another, meaning the device accurately traced the movement of water currents at depth without
30 undue influence of wind and waves. Each device cost USD \$265 in 2021 and was built from
31 materials readily available at hardware and sporting goods stores, allowing their use by research
32 institutions and communities with smaller budgets. This design reliably measured lake currents
33 at sampling depths that ranged from 2 m to 30 m. We anticipate that this design will have
34 application to a wide range of hydrodynamic and ecological research where empirical insights to
35 physical processes like lake currents are sought by scientists and managers.

36 **Plain Language Summary**

37 Lake currents are complex, yet often lack data for scientists to analyze them. We built and tested
38 a low-cost, accurate device that can follow water currents in lakes, made from easily available
39 parts. Unlike similar devices for oceans which can be bulky and costly, this device is well-suited
40 for lakes. It works by floating on the water's surface and has a part that hangs below it in the
41 water to track water movement at different depths. Tests in two New York lakes showed it does a
42 great job of tracking water without being thrown off by wind or waves. Making each device
43 costs \$265, using parts found in regular stores, so it's affordable for smaller research teams or
44 local communities. It's good for studying water movements from near the surface down to 30
45 meters or even deeper, helping scientists and local managers learn more about how water moves
46 in lakes.

47

- 48 **Keywords** (up to 5 words)
- 49 Lakes, currents, Lagrangian, drifter

50 **1 Introduction**

51 Reliable measurements of currents in inland lake settings are often lacking, despite the
52 potential for lakes to provide an equally dynamic setting relative to larger water bodies. For
53 example, lake currents are a function of complex processes that may include highly variable
54 wind inputs, river inflows, and variable bathymetry and morphological characteristics (Hutter et
55 al., 2011; Wetzel, 2001). Understanding such physical characteristics in lakes is crucial to shed
56 light on physical, sedimentological, chemical, and biological processes that define the
57 environmental health of the system. Currents have historically been investigated in marine
58 settings using a variety of robust and capable sampling equipment, though often expensive and
59 difficult to deploy (Edwards et al., 2006, and references therein). Currents in the Laurentian
60 Great Lakes of North America and similar large lakes (Choi et al., 2020; Edwards et al. 2006), in
61 the coastal zone (Sabet and Barani, 2011), and in estuaries (Spencer et al., 2014; Suara et al.,
62 2018; Déjeans et al., 2021) have also been investigated, yet smaller and medium-sized lakes
63 (~50-500 km²) have received less attention than perhaps they should have, despite improvements
64 in technology including the availability of small GPS units as tracking devices (McCormick et
65 al., 2006; Manley, 2010). New technology and low-cost, high-performance materials are
66 therefore unlocking opportunities to measure currents in a wider range of water body sizes,
67 including smaller inland lakes. Here, we developed an economical Lagrangian drifter design
68 assembled from readily sourced materials, and we validated its research potential with field
69 deployments in the Finger Lakes region of New York State, USA.

70 Lagrangian drifters are devices used to directly trace currents at a discrete depth interval
71 while minimizing the influence of wind and currents at the surface (Booth, 1981). They contrast
72 with Eulerian-type sensors such as Acoustic Doppler Current Profilers (ADCP), which are
73 usually moored to the bottom of a waterbody where they measure velocity at multiple depths
74 through the water column. Lagrangian drifters comprise of a low-drag surface float containing
75 positioning and communication equipment, and a high-drag drogue tethered beneath the float.
76 Alternatively, drifters specifically designed for surface measurements have only a high-drag
77 float. Commercial options for surface drifters vary in design and construction and include the
78 CODE drifter (Davis, 1985) and the drifter design of Meyerjürgens et al. (2019). The CARTHE
79 drifter (Novelli et al., 2017) is unusual in that it is a biodegradable surface drifter with a drogue
80 suspended by a short chain directly underneath the float to address tilting of the device in large

81 waves and modification of its current-attributed motion. Drifter designs for oceanography and
82 Great Lakes research have evolved from TRISTAR (Mackas et al., 1989) and CODE drifters to
83 the Surface Velocity Program ('SVP') drifters: (Sybrandy & Niiler, 1992; Lumpkin & Pazos,
84 2006; Poulain et al., 2022). SVP drifters have a cylindrical cordura nylon fabric drogue of 0.6 m
85 diameter which extends vertically around 20 m, centered at a depth of 15 m. Ocean-going
86 drifters are robust platforms for data collection, as they are designed to withstand rough ocean
87 conditions and to transmit their location and environmental data for several months up to a
88 decade. Accordingly, they range in cost from around USD\$1800 for the basic structure to many
89 thousands of dollars for fully instrumented drifters, which can be cost-prohibitive depending on
90 the research setting (<https://www.aoml.noaa.gov/phod/gdp/faq.php#cost>, accessed 17 February
91 2023).

92 A drifter to be used on freshwater lakes (global mean depth 42 m; Cael, 2017) has
93 differing requirements to ocean-going drifters (global mean depth 2660 m; Charette & Smith,
94 2010). Seasonal stratification and proximal flow boundaries (shoreline and lake bottom) mean
95 that the vector of currents will differ vertically through the relatively shallow water column and
96 over short time intervals of hours to days. The smaller extent of freshwater lakes compared to the
97 oceans and the greater risk of grounding in shallow water compared to ocean-going drifters
98 entails a shorter deployment duration, smaller battery capacities, but also a higher chance of
99 encountering commercial or recreational vessels. A shorter mean fetch resulting in lower
100 amplitude waves suggests that the design need not be as robust as ocean going drifters,
101 decreasing material requirements, cost, and vessel size required for deployment and retrieval.
102 Depending on the lake, we anticipate a higher chance of easy deployment and certainty of
103 recovery using a transmitted GPS position, meaning that practical and cheap onboard logging of
104 environmental sensor data is a viable alternative to telemetry. These factors and many studies
105 (e.g. Gasser et al., 2001; Austin & Atkinson, 2004; Cadena et al., 2018; Agade & Bean, 2023)
106 suggest that oceanographic designs are over-engineered for measuring currents in small to
107 medium-sized lakes, and thus needlessly expensive. Although drifters for smaller waterbodies
108 have been described (Mullarney & Henderson, 2013; MacDonald & Mullarney, 2015; Fuentes-
109 Pérez et al., 2022 Table 1), many are optimized for specialist data collection (e.g. ADCP, video),
110 are expensive, or incorporate proprietary designs that are not easily replicable.

111 Here, we demonstrate how a novel Lagrangian drifter design can provide reliable
112 empirical insights to deep currents in freshwater inland lake settings. The drogue design was
113 tested in lakes in the Finger Lakes region of New York State, USA, and provided sufficient
114 information to evaluate local circulation patterns at relatively deep depths in waterbodies with
115 much smaller surface areas than in the oceans and Great Lakes. The objectives of this study were
116 to: 1) Design and construct a new, easily assembled, deployable, and retrievable, and open-
117 source, economical Lagrangian drifter specifically for small to medium-sized lake settings, 2)
118 estimate forces of drag on the design to ensure movement is a function of currents, 3) validate
119 the drifter design through field deployments, and 4) obtain empirical measurements of lake
120 currents with the instrument. For USD\$265 (in 2021 costs) the drogue design met all criteria
121 necessary for ease of deployment and reliable current measurement in deep water. We thus
122 believe this design could broaden the availability of such drifters to research programs and
123 communities with lower budgets and may have important applications in the water resources
124 community.

125 **2 Materials and Methods**

126 2.1 Drogue Design

127 Our drogue design (**Figure 1**) consists of three square planes of High-Density Polyethylene
128 (HDPE, density 915 g/L) arranged orthogonally, dimensions of width, breadth and height of 1.22
129 m (4 ft; 1.72 m diagonally), and joints cinched with cable ties (also known as ‘zip ties’, nylon, 20
130 kg breaking strength). Critical points such as the attachment point of tether to drogue had
131 multiple zip ties to ensure redundancy. Each plane is built from four smaller panels of dimension
132 0.61 m (2 ft), which, with judicious folding, enables its easy transportation and later ability to
133 reform prior to deployment. HDPE is stiff even when thin (2 mm), chemically inert, abrasion
134 resistant, and with a finish that discourages encrustation, e.g., in our study system, encrustation
135 by invasive *Dreissenid* mussels. Drifters were deployed with Hobo MX2201 temperature loggers
136 attached to a drogue panel. Steel weights (1 – 3 kg) attached to the bottom of the drogue via zip
137 ties were used to overcome drogue buoyancy and decrease the possibility of wind and wave
138 rectification and lateral translation, and also enabled the cylindrical floats to remain upright. The
139 design of drifter is a modification of that of Manley (2010), but differs in significant aspects

140 (horizontal drogue plane, HDPE drogue material, use of Globalstar satellite system and SPOT
141 Trace GPS units, and solar powered top beacon).

142 2.2 Float Design

143 The float design (**Figure 1b**) takes the form of a resealable buoy, comprised of Polyvinyl
144 chloride (PVC) cylindrical tubing and end caps. PVC is inexpensive, robust, easy to fabricate
145 and glue, and readily available. The float is approximately 0.6 m long, external diameter of 0.089
146 m (3.5 inches), filled with closed-cell foam to mitigate against leaks or damage. A 0.05 m (2
147 inch) eye bolt is mounted through the lower cap, secured in place with nuts and washers, and
148 cemented in place with silicone sealant to prevent leaks. Approximately 0.1 m of the float is
149 above water, plus whatever high-visibility beacon is attached. The top section is sealed via a
150 water-tight thread, allowing access to a compartment for Global Navigation Satellite System
151 (GNSS) device storage. We used SPOT Trace GPS units ([https://www.findmespot.com/en-](https://www.findmespot.com/en-us/products-services/spot-trace)
152 [us/products-services/spot-trace](https://www.findmespot.com/en-us/products-services/spot-trace), 6.8 cm × 5.1 cm × 2.1 cm, purchased 2021 and 2022) equipped
153 with high-grade lithium batteries within the top compartment (**Figure 1c**), which transmit
154 location via the Globalstar satellite network with options to program transmission frequency
155 between 150 seconds and 1 hour. The upper cap screw-in surface has a solar-powered flashing
156 beacon to aid in retrieval and avoidance of collisions. The tether was 3 mm braided nylon
157 (breaking strain 50 kg), with an additional 1 m of elastic shock cord. This was needed because
158 without elasticity in the tether system the vertical stability of the drogue in the water column,
159 combined with the buoyancy of the float, could induce high dynamic loads on an inelastic tether
160 in high wave conditions. Materials for each drifter cost around USD \$265 in 2021, plus USD
161 \$30/month for GPS service subscription. Construction time is around three hours per drifter. A
162 complete parts list and construction manual are available in Supporting Information (see Section
163 **SI1**).

164

165

166

167

168

169

170

a)

b)

c)



171

172 **Figure 1.** Component parts of the drifter. Drifter design comprises of **a)** High-resistance drogue
173 of three orthogonally-arranged HDPE plates each with a dimension of 1.22 m (4 ft) and **b)** Low-
174 resistance foam-filled PVC float approximately 0.6 m in length, joined by a tether (not shown).
175 The float top cap, **c)**, is removable to access the SPOT Trace GPS unit, which sits on top of a
176 rubber gasket secured in place with silicone sealant. Steel weights are added to balance
177 buoyancy.

178

179

2.3 Establishing Water-following Characteristics

180

We used four methods to test the influence of the float on drogue movement:

181

1) Theoretical calculations of drag ratio based on drag coefficients and cross-sectional area;

182

2) Experimental measurement of drag forces on float and drogue at differing water velocities;

183

3) Graphical analysis of data from the deployment of drifters on Seneca and Keuka Lakes,

184

showing drifter versus wind vectors; and

185

4) Statistical analysis of wind and drifter direction using both linear regression and Kendall's

186

rank coefficient between hourly wind and drifter bearings.

187

2.3.1. Theoretical Drag Forces

188

A required design characteristic for a drifter is the tendency of the drogue to follow a water

189

parcel while minimizing influences on the movement vector by other factors such as wind and

190

surface gravity waves. The drag coefficients, C_D , of specific shapes (Nakayama 2018) is used

191 with the dimension, A, of components of this and other drifters (**Table 1**) to calculate the drag
192 area, $A_D = C_D A$, for the drogue and float, to arrive at a drag area ratio, R,

$$R = A_D^{drogue} / A_D^{float}$$

193 A large value of R (ratio of drogue/float drag areas) is desired, and a coefficient of 40 is
194 described as a minimum for Lagrangian drifter devices (Niiler et al, 1996).

195 2.3.2. Experimental Drag Forces

196 Experimental measurement of forces due to drag were carried out either by: 1) Dragging the
197 components sideways alongside a dock in static water, 2) pulling upwards from the bottom of a
198 swimming pool, both at varying low (<0.5 m/s) velocities, or 3) by towing full-size drifter
199 components from a boat (>0.5 m/s), while measuring the resultant force with a digital strain
200 gauge (read in kg, converted to newtons; 1 kg = 9.81 N). Vertical and horizontal methods of
201 drogue and float drag measurement were deemed equivalent because of the symmetry of the
202 devices in three dimensions, and the forces induced by dragging either vertically or horizontally
203 are much greater than those generated by those induced by sinking. In a lake, the components are
204 never likely to experience these speeds through the water: the experiment is only to show the
205 drag area ratio at a variety of speeds. The float was filled with water to approximate neutral
206 density, and during experiments it was completely submerged; the force reported here is that
207 experienced by the length of float below the surface during deployment (0.5 m). Drag force (F_d)
208 is proportional to surface area A, square of the velocity V, density of fluid ρ , and drag
209 coefficient C_D ,

$$F_d = \frac{1}{2} \rho v^2 C_D A$$

210
211 meaning that drag force ratios are better approximated using regressions expressed as a power, in
212 the form of $y=ax^b$. Power regression lines were fitted to the data for each component. Drag area
213 ratio at each velocity is equivalent to the difference in slope between fitted lines.

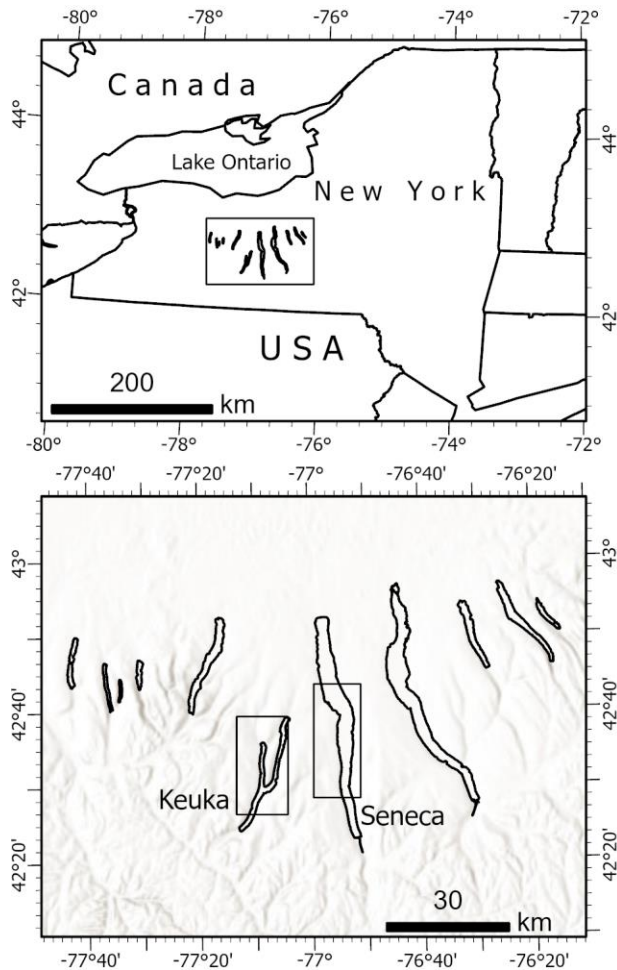
214 2.3.3. Field Deployment

215 *Study system*

216 The drifter design was tested in the Finger Lakes region of New York, USA (**Figure 2**) in
217 October 2021 and October 2022. The Finger Lakes are glacially-formed (Mullins et al. 1996),

218 elongate lakes oriented approximately north-south. All lakes drain northward into Lake Ontario
219 within the Laurentian Great Lakes basin. Wind directions are often parallel to their long axes,
220 resulting in the generation of surface and internal seiches (Ahrnsbrak 1974). We specifically
221 deployed drifters in Seneca Lake and Keuka Lake (the latter is detailed in Supplemental
222 Information, **S2**). Each lake is monomictic with strong seasonal thermoclines that persist until
223 mid to late Fall (northern hemisphere Autumn). Seneca Lake has a simple morphology –
224 essentially bathtub-shaped, with steep east and west sides, shoals at the north and south ends, and
225 a mostly flat bottom. ADCP data over a 10-day period in 2018 at a northerly site in Seneca Lake
226 (USGS, in prep) indicated currents had a maximum velocity of 0.43 m/s, although 95% (± 2
227 standard deviations) were less than 0.3 m/s. This is in line with the author’s (LM) personal
228 experience when conducting lake profiles, that equipment being lowered into the lake on a calm
229 day with no boat drift can be pulled strongly in various directions. No measurement has been
230 made of current strength in the central section of the lake, where seiches might be expected to
231 generate the highest velocity currents.

232



233
 234 **Figure 2.** *Top*) Location of the Finger Lakes within New York State, USA, and *Bottom*) the
 235 Finger Lakes region, highlighting Seneca Lake and Keuka Lake, the sites of experimental
 236 deployments of this drifter design in Fall 2021 and Fall 2022. Boxes indicate areas of drifter
 237 movement during deployment.

238
 239 *Drifter configuration and deployment*

240 Drogues were transported to deployment locations on boats folded upon themselves in one plane,
 241 then planes were unfolded and fixed in position either on shore or, space and wave conditions
 242 permitting, just before deployment from the boat. Drogues were deployed first, followed by
 243 tether, and then the float once the drogue reached sampling depth. Deployment took about five
 244 minutes with two people. Upon release we ensured, by the addition of extra ballast on the drogue
 245 if needed, that floats were vertical and there was no slack in the tether. We validated that all GPS
 246 devices were logging GPS coordinates upon their release.

247 Positions of the floats are transmitted via satellite to a data center; a subscription-based,
248 shareable online map of last known and historic positions available through SPOT
249 (<https://www.findmespot.com/en-us/>). We configured this map to a public setting and found that
250 we increased local community participation during our lake experiments. Additionally, GPS
251 points are available from SPOT at the time interval configured (e.g., 10-minute rate), which can
252 be viewed via smartphone to enable drifter recovery if sampling in an area with cell reception. At
253 night, the flashing beacon was also highly visible, even in choppy water. For instance, one SPOT
254 Trace unit suffered a battery failure at nine days during the Seneca lake deployment, but the
255 drifter was eventually retrieved via a social media campaign which led to multiple reports from
256 shoreline residents of the flashing beacon at night. Retrieval of all other drifters was easily
257 accomplished despite up to a 10-minute delay on position location. Upon retrieval, we observed
258 no modification to the drogue and float design throughout deployment, including no zip tie
259 failures, no water entry into the float, or degradation of the nylon tether.

260 *Data processing*

261 Latitude and longitude data for each drifter were downloaded from the SPOT website after
262 drifter recovery, then converted to comma delimited files for processing. Wind and drifter data
263 frequency was aggregated hourly using the Pandas Library (version 2.1.4; McKinney, 2010) in
264 Python (version 3.9.13; Python Software Foundation 2024). All statistical analyses presented
265 here used SciPy (version 1.12.0 2024-01-20; Pauli et al. 2020). Velocity between each location
266 fix was calculated using the haversine formula (Van Brummelen, 2013) from sequential latitude
267 and longitudes transmitted by the GPS units. Grounding of the drifter on the lakebed was
268 indicated initially by a decrease in speed and localization of the drifter over several hours, and
269 subsequently confirmed by a comparison of the drogue depth with bathymetric data. Vectors
270 while the drifters were grounded and being relocated to a deeper water location were set to ‘null’
271 in files for analysis.

272 For deployment on Seneca Lake, wind speed was measured at a buoy (42°49'07.8"N,
273 76°57'36.6"W, 17km from the initial deployment location, 3.1m elevation above water) off Clark
274 Point, using a RM Young 05106 instrument (wind speed accuracy of 0.3 m/s, wind direction
275 accuracy of 3°, downloaded from <http://fli-data.hws.edu/buoy/seneca/>).

276

277 **3 Results**

278 3.1 Theoretical Design Validation

279 The R value for our float-drogue combination is around 90, 39% less than the R-value of the
 280 SVP-B drifter design (~140). The SVP-B drifter could be considered the ‘gold standard’ because
 281 of its ubiquity in oceanic drifter studies. The drag due to the tether is approximately 0.0022 N/m
 282 and has been ignored in the following calculations, given that all designs considered here have
 283 tethers.

284
 285 **Table 1:** Dimensions and drag coefficients of this and other drifters. Drag coefficients from
 286 Nakayama (2018). SVP-B dimension from Sybrandy and Niiler (1992) and Lumpkin and Pazos
 287 (2006). Johnson drifter dimensions are from figure and text descriptions in Johnson et al. (2003)
 288 and CARTHE drifter dimensions are from Pacific Gyre (2023).

289

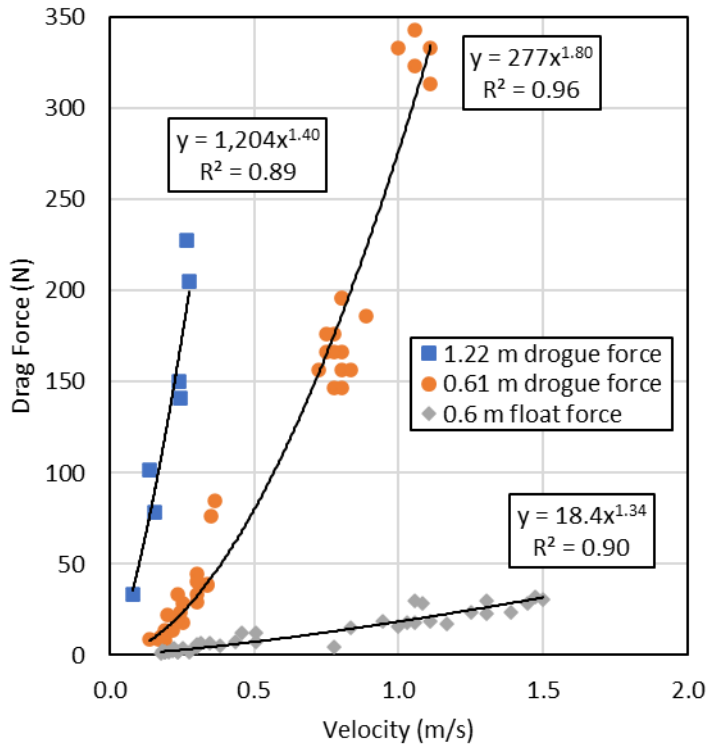
	This study	SVP-B	Johnson	CARTHE
Float submerged cross section A (m ²)	0.044	0.040	0.032	0.023
Float form	Cylinder	Hemisphere	Cylinder	Toroid
Drag Coefficient C _D	0.74	0.42	0.74	0.42
Float drag area A _D ^{float}	0.033	0.017	0.024	0.010
Drogue Dimensions (m)	1.22 x 1.22	0.61 x 4.9	0.63 diameter	0.38 x 0.38
Drogue Cross section A (m ²)	1.49	2.99	0.31	0.14
Effective drogue form	Flat plate	Cylinder with holes	Hemisphere, type II	Flat plate
Drag Coefficient C _D	1.98	0.74	1.33	1.98
Drogue drag area A _D ^{drogue}	2.95	2.45	0.41	0.286
Drag Area Ratio, R	89	146	17	28.6

290

3.2 Experimental Design Validation

For experiments measuring actual forces on drifter components, forces increased predictably, whether the experiment was conducted at low speed (dockside/pool) or towed behind a boat (**Figure 3**). Initially approximating the drag forces as simple linear regressions, the submerged area of float (0.5 m length) induced a drag of 21 N/m/s whereas a 0.61 m drogue (width, length, and height) induced a drag of 316 N/m/s, equivalent to a drag area ratio of approximately 15 (316/21 N/m/s), below the minimum required value of 40 (Niiler et al, 1996). Experiments with a 1.22 m drogue showed that drag forces were much higher (855 N/m/s), although not four times higher than the 0.61 m drogue, as might be expected from the increase of surface area by four times. These experiments confirmed the requirement to use larger drogues. In theory, all fitted regression lines should pass through the origin since there should be no drag at zero velocity, but we analyzed our experimental dataset as empirical, non-corrected data.

In order to determine when the ratio of drag forces between y^d (1.22 m drogue, $y^d=1204.62x^{1.4}$) and y^f (float, $y^f=18.37x^{1.34}$) meet the value of 40 stated in Niiler et al (1996), we set $y^d=(40)y^f$. In doing so we get $1204x^{1.4} = (40)18.4x^{1.34}$. When solved algebraically, $x=0.0026$ m/s, meaning at this velocity the drag ratio of y^d (drogue) to y^f (float) is 40. At velocities greater than 0.00026 m/s, the ratio will be greater than 40, as the drag force of y^d increases at a greater rate than the drag force of y^f , as the exponent of y^d is greater than the exponent of y^f .



310
 311 **Figure 3.** Drag forces on full-size drifter components. Values below 0.5 m/s were measured
 312 either at a dock or a swimming pool, those above 0.5 m/s were measured from a moving boat.
 313 Float was filled with water to achieve approximately neutral buoyancy. Equations for the power
 314 regression lines are given along with R^2 values for the best fit.

315

316 3.3 Field Experiments

317 We field validated the drifter design on two medium-sized inland lakes of up to 180 m depth and
 318 17,000 ha (66 mi²) in area (**Table 2**). We found that drifters moved up to several kilometers per
 319 day and GPS units successfully tracked location without important data gaps. Velocity and
 320 distance covered by drifters in the epilimnion (20 m deep) were greater than in the relatively
 321 thicker hypolimnion (120-160 m thickness).

322

323

324

325

326 **Table 2:** Deployment details for the current design on two Finger Lakes. The total deployment
 327 time is the sum of all drifter deployment durations, and includes time grounded or being
 328 redeployed to deeper water. Further details of the Keuka Lake deployment are found in
 329 Supplemental Information Section S2.

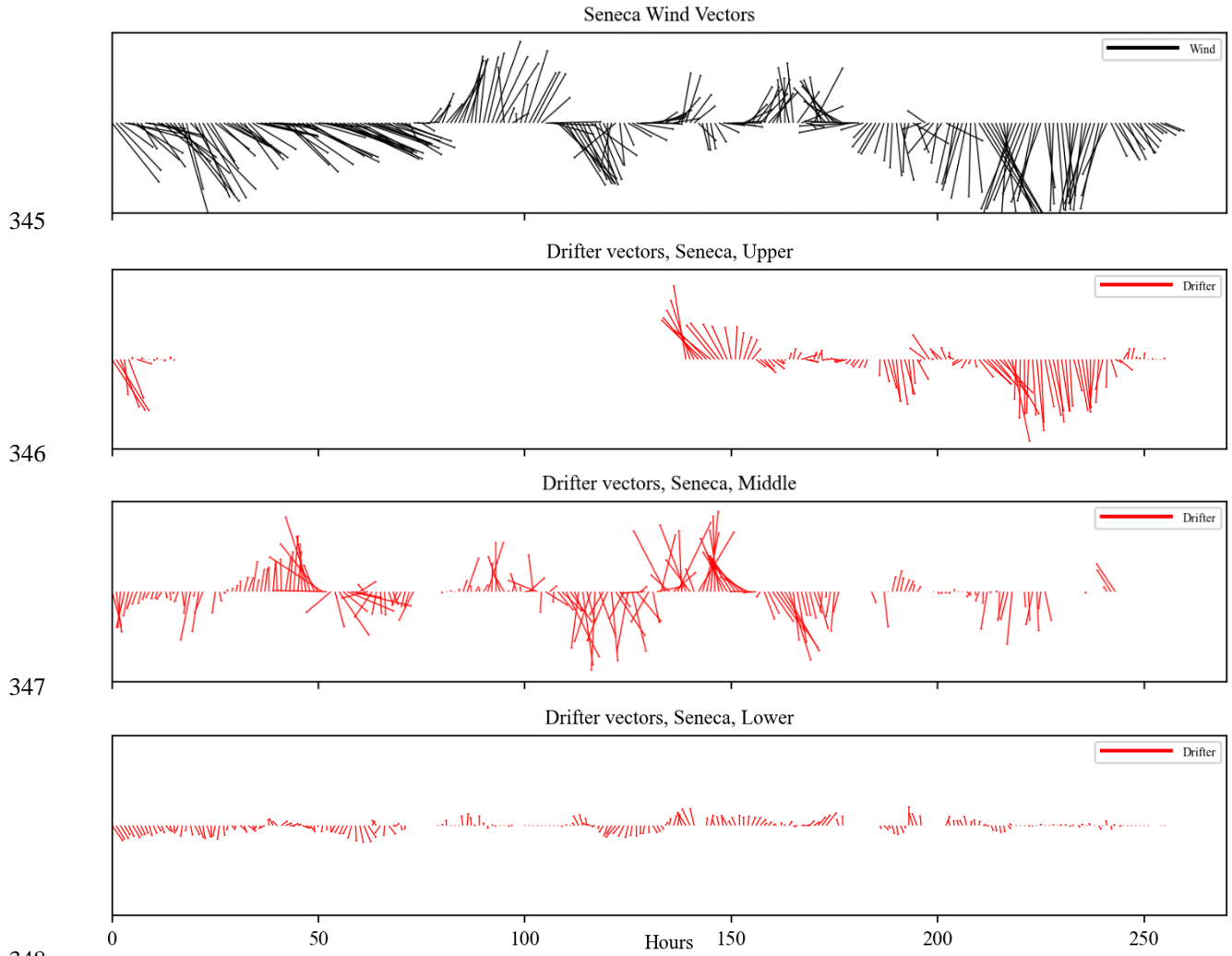
330

	Seneca Lake	Keuka Lake
Area (hectares)	17,540	4,688
Maximum depth (m)	188	56
Length (km)	61	31.5
Deployment Date	17 October 2021	30 September 2022
Number of drifters	3	6
Total deployment time (drifter-hours)	768	2734
Location frequency (minutes)	5	10

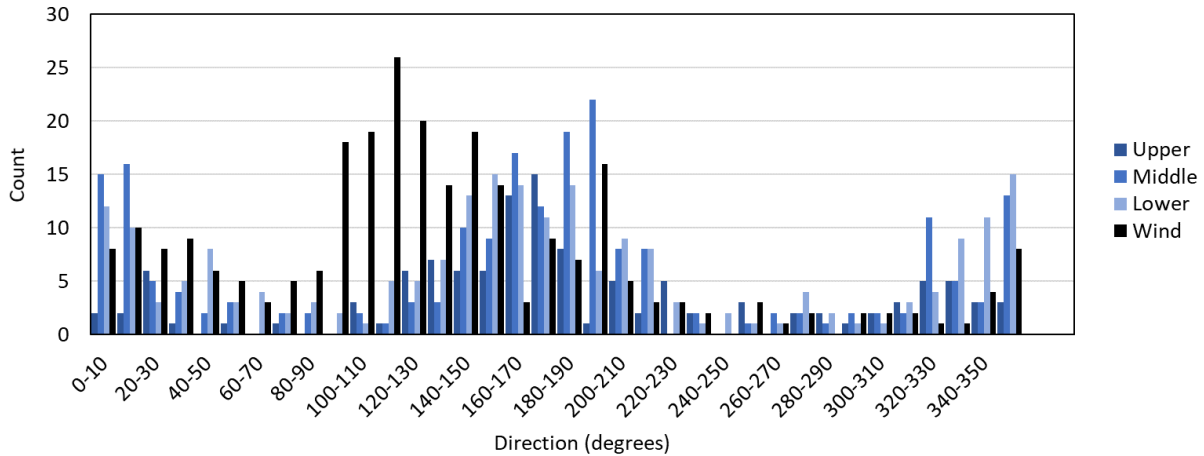
331

332 **Case Study: Seneca Lake**

333 Three drifters were deployed in Seneca Lake for 10-14 days in October 2021. They were
 334 configured for three levels: 2 m, 10 m, and 30 m ('Upper', 'Middle', and 'Lower', respectively).
 335 The Upper drifter had a 0.61 m wide drogue, whereas the Middle and Lower drifters had 1.22 m
 336 wide drogues. Wind and drifter vectors were plotted against time to illustrate the degree of
 337 coherence between the two data types (**Figure 4**). Mean drifter speeds were 0.15 m/s, 0.10 m/s
 338 and 0.025 m/s for Upper, Middle, and Lower drifters respectively, compared to 4.95 m/s for
 339 wind speed. Typically, winds are described in terms of the direction they are coming from, but
 340 wind directions and vectors in this paper refer to the direction the wind is going *towards* for
 341 easier comparison with the drifter information. Wind was predominantly towards ESE to SSE,
 342 and drifter movement was predominantly to N or S (**Figure 5**). Some degree of agreement
 343 between wind vector and Upper drifter vector is apparent but is not for Middle and Lower
 344 drifters.



348
 349 **Figure 4.** Comparison of hourly wind vectors with those of Upper, Middle, and Lower drifter
 350 vectors, Seneca Lake, New York, USA from 17 October 2021 to 28 October 2021. The origin of
 351 each vector line is marked horizontally in hours from the start of deployment. Length of line is
 352 proportional to velocity, and direction of the line from its origin represents the direction towards
 353 which the wind/drifter was moving. Velocity scale is proportional to the line length in the
 354 legend: Wind, 0 to 7.2 m/s; drifters, 0 to 0.3 m/s. The scale has been adjusted (x24 exaggeration
 355 for visualization) between wind and drifter plots to allow easier visual comparison. Gaps in date
 356 are due to either grounding or failure to receive a positioning signal.
 357



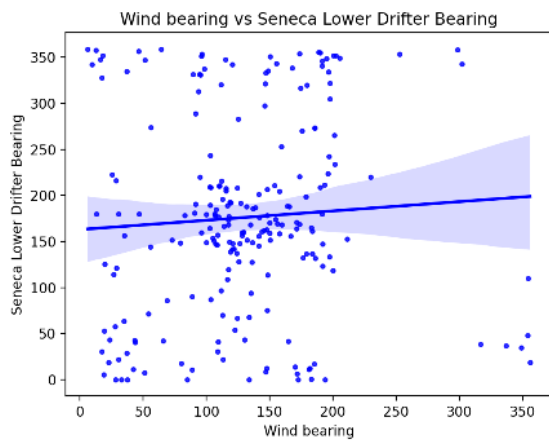
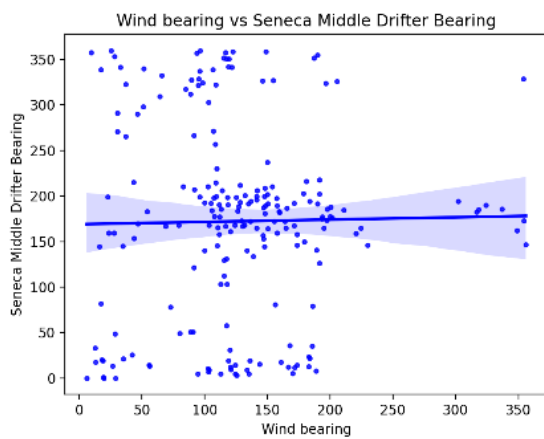
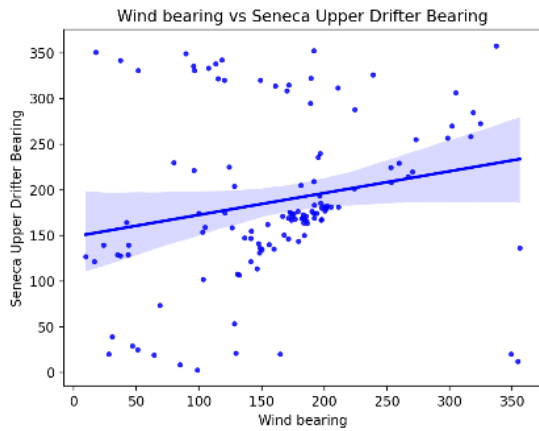
358

359 **Figure 5.** A histogram of wind and drifter direction over the course of experimental deployment
 360 (17 October 2020 to 27 October 2020) on Seneca Lake, New York, USA.

361

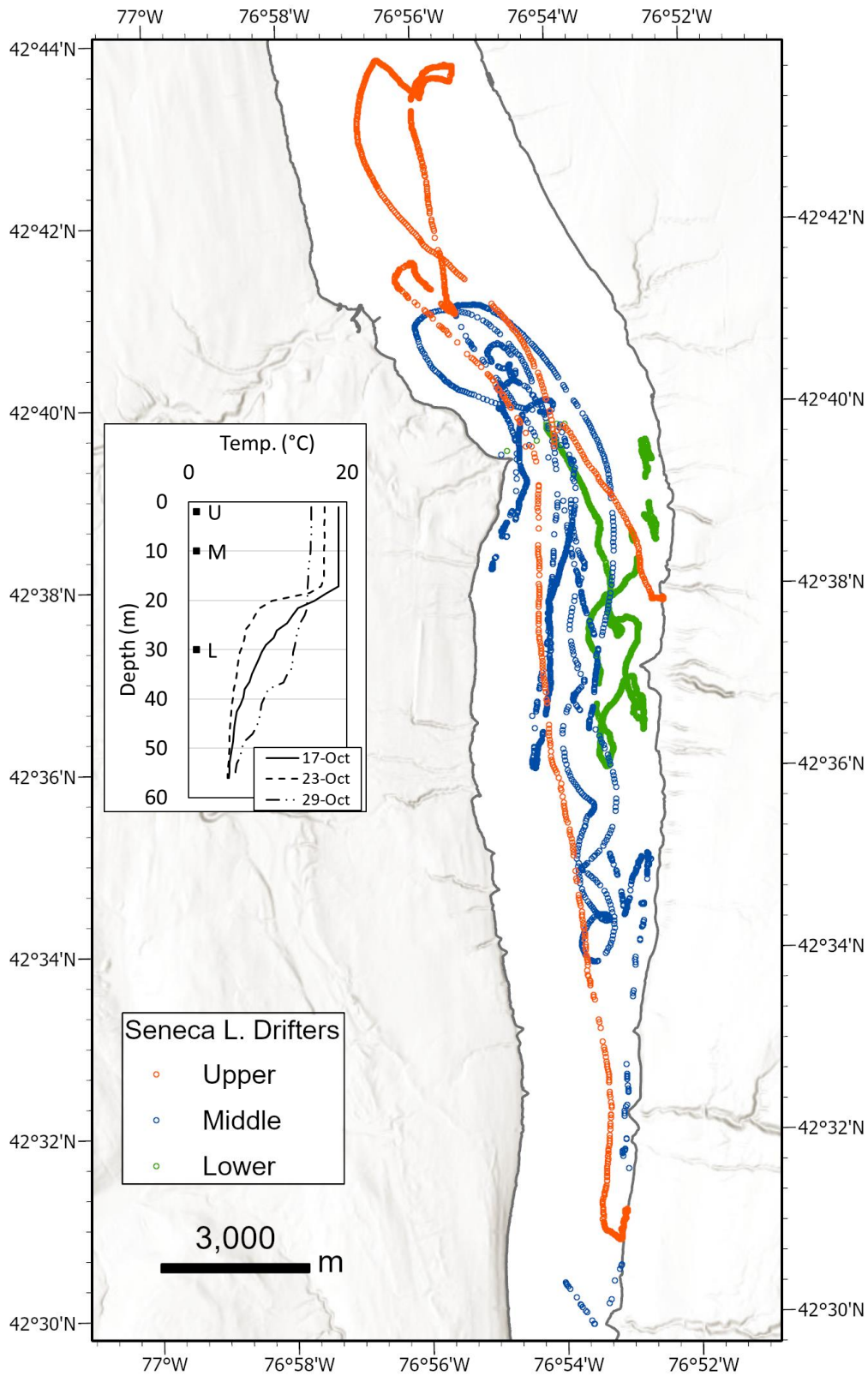
362 A linear regression of wind and drifter hourly bearings indicated low coefficients of
 363 determination (R^2) for Upper, Middle, and Lower drifters of 0.0439, 0.0003, and 0.004,
 364 respectively (**Figure 6**). Spearman rank correlation coefficients (τ) for hourly wind direction and
 365 Upper, Middle, and Lower drifter bearings indicated that middle and lower drifter direction of
 366 movement was unrelated to wind direction ($\tau = -0.0279$ and 0.0813 , p values = 0.5487 and
 367 0.0743 , $n = 209$ and 218 , respectively). Upper drifter direction was weakly correlated to wind
 368 direction ($\tau = 0.3391$, p -value = 0.01 , $n = 116$). Drifters moved many kilometers over the
 369 duration of deployment (**Figure 7**). Velocities aggregated over half an hour provide velocity
 370 estimates down to 0.02 m/s, based on the stated accuracy of the GPS system of ± 5 m horizontal.

371



372 **Figure 6.** Comparison of hourly wind bearings with a) Upper, b) Middle, c) Lower drifter
 373 bearings while deployed on Seneca Lake, New York, USA from 17 October 2021 to 27 October
 374 2021. The solid blue line is linear regression model fit, with shaded areas indicating 95%
 375 confidence interval band.

376



377

378 **Figure 7.** Drifter positions on Seneca Lake, 17-27 October 2021. Inset: Thermal profile and

379 drifter depths ('U', 'M', 'L' = Upper, Middle, and Lower drifters, respectively).

380 **5 Discussion**

381 This study integrates multiple calculations and field-based testing to validate a novel Lagrangian
382 drifter design. Experiments reveal that this design exceeded drag force thresholds between the
383 suspended drogue and surface float, which indicates that movement of this device through the
384 water column is a function of lake currents. Through extensive field deployments, we found that
385 the design reliably measures deep current characteristics of direction and velocity in deep inland
386 lakes. By deploying our drifter design at scale, we demonstrate that this cost-effective, reliable
387 design provided information useful for elucidating current patterns in lakes that have previously
388 lacked measurements of deep currents.

389
390 The present drifter has a theoretical $R = \sim 80$, double the minimum value of 40 suggested by
391 Niiler et al. (1995). Theoretical calculations of the float and drogue drag and several drifter
392 designs documented in the literature (**Table 1**) show a range of drag area ratios, R , from about 17
393 for the Johnson et al. (2003) design to over 140 for the SVP-B design. The high R value for the
394 SVP-B design is primarily due to the high cross-sectional area (particularly in the depth
395 dimension) of the SVP-B ‘Holey Sock’ drogue. This large interval of measurement depth may
396 not be a significant problem in oceanographic studies, but in a lake, current vectors may change
397 over much shorter depth intervals. We note that the drifter of Johnson et al (2003) is comprised
398 of a drogue using an 85-liter bucket. The stated drogue surface area of 2.25 m^2 is quite possible,
399 but the cross-sectional area of a standard bucket, which is the relevant dimension for drag
400 calculations, would vary between 0.17 and 0.31 m^2 depending on orientation to water flow. The
401 resulting drag area ratio of the Johnson drifter using realistic drag coefficients at the high end of
402 drogue cross-sectional area is well below 40. The CARTHE drifter has a theoretical R value
403 around 29, despite the relatively modest size of its drogue, likely resulting from the notably low
404 cross-sectional area of its toroidal float. Extensive lab measurements of the CARTHE drifter
405 (Novelli et al. 2017) found it to have excellent water-following characteristics. We found it
406 difficult to select the appropriate shape type from the available hydrodynamic drag literature,
407 since none of the drogue configurations were present in existing literature (orthogonally arranged
408 plates, cylinder with holes, bucket, and sideways-toroid). The reported drag values are
409 conservative estimates based on the shapes of each drogue configuration – when unavailable or
410 uncertain, we chose values to increase the value of R in other drifter systems.

411 Experimental measurement of drag on full-sized components confirmed the drag ratio of float to
412 1.22 m drogue was above 40, but only marginally. The 0.61 m drogue data is scattered at higher
413 velocities, which fits with field observations of the difficulty of measuring those higher forces
414 from the back of a boat. To the authors' knowledge no equivalent tests have been performed on
415 other drifters, and it would be illuminating to see what the results of such experiments would be.
416 However, this experimental approach to measurement of drag ratio may not be suitable for
417 drogue designs which lack a method to prevent slippage when deployed in anything other than a
418 vertical orientation, or those which would deform or collapse if subjected to lateral forces.

419
420 The graphical comparison of wind and drifter vectors over time lends support to the
421 independence of the two vectors, particularly for middle and deep drifter deployments on Seneca
422 Lake, and for all the drifters deployed to Keuka Lake. The speed and direction of the wind is
423 often seen to disagree with the speed and direction of the drifters. In a mental exercise, one could
424 imagine that if the two sets of vectors were in fact random and uncorrelated, they would still
425 roughly coincide for some fraction of time. In the case of the experimental deployment, wind and
426 drifter vectors do indeed coincide for part of the time. Drifter direction is limited by the roughly
427 N or S movement of currents along the longitudinal axis of the two study lakes, while wind
428 direction is at times modified from blowing towards eastern and northeastern direction by the
429 funneling effect of the topography, modifying it towards the north along the lakes. The slightly
430 increased value of Spearman rank coefficient for the Seneca Lake Upper drifter (with a smaller
431 0.61 m drogue set at 2 m depth) may be due to wind-induced movement in the top couple of
432 meters but is most likely caused by an insufficient drag coefficient ratio. A comparison of drifter
433 velocity data provided by SPOT, with velocity calculated from latitude and longitude indicates
434 that SPOT velocities are not provided at very low speeds, possibly because of a threshold set in
435 the SPOT reporting system.

436
437 The low values of the wind/drifter direction Spearman rank correlation coefficient confirm
438 independence of these parameters. Drifters moved mostly north or south (longitudinally) in
439 Seneca Lake, possibly due to internal seiche-induced currents. Temperature spikes detected and
440 recorded by the attached HOBO sensors coincided with change in movement from north to
441 south, suggesting passage of an internal wave. When drifters moved east or west (laterally) they

442 were caught in a gyre, or about to change from north to south or vice versa. The drifter direction
443 of movements on Keuka Lake was more complex, with one drifter ('East Shallow') eventually
444 making its way into all three branches of the lake, against the prevailing wind direction (see
445 Supplemental Information **Section S2** for further details).

446
447 Our practical drifter design has the potential to be deployed at scale in inland lakes with
448 implications for both basic and applied research questions. For example, small and medium-sized
449 lakes have been the focus of research on water quality issues worldwide, particularly resulting
450 from a perceived increase in harmful algae blooms (Ho et al. 2020). Surface currents have been
451 suggested as significant transport mechanisms for harmful bloom-forming cyanobacteria
452 (Ishikawa et al. 2002), and deep currents have been suggested as a source of turbulent upwelling
453 of nutrients (Bourgault et al. 2014) so an improved understanding of the scale, frequency and
454 movement of lake currents could be a useful contribution to the study of blooms. The use of the
455 design could enable harmful algae bloom forecasting based on hydrodynamic models (see
456 Wynne et al. 2013) to be improved with empirical current data against which a model could be
457 calibrated and validated (Mardani 2020), as an alternative or in addition to data from ADCP and
458 thermistor strings. This economical drifter design also has potential for integration into
459 ecological sampling methods such as environmental DNA (eDNA), a technique to detect the
460 presence and distribution of aquatic organisms (Deiner et al. 2017; Beng and Corlett 2020)
461 whereby current data can provide further insight to DNA particle transport in lake surveys. The
462 design may provide lake scientists with datasets that bridge the gap between currents predicted
463 by hydrological models and empirical, field-based measurements.

464

465 **6 Comments and Recommendations**

466 We conclude that the design when using 1.22 m drogues meets or exceeds the minimum
467 suggested drag area ratio between surface float and drogue. The water-following characteristics
468 of the present design are sufficient to suggest that this design is a true Lagrangian drifter in the
469 horizontal plane, with minimal influence from wind or wave action. The simple and robust
470 design is economical, easy to construct, and convenient to deploy and recover. The open-source
471 drogue design can be assembled from components generally available at local hardware or

472 sporting goods stores, without the need for proprietary material. We demonstrated that our
473 design successfully collected field measurements of deep currents in inland lake settings and
474 believe that this design can be applied economically to the broader water resources field to
475 further shed light on deep currents.

476

477 **Acknowledgments**

478 The authors thank Birdem Oz and Jacob Stewart for help with construction, testing and
479 deployment of early prototypes; Andrew Hagen for boat loan for component testing on
480 Skaneateles Lake; Carl St. John and Susan Ball for assisting with component testing in the pool;
481 Dan Corbett and Larry Martin for Seneca Lake deployments and recovery. For the Keuka Lake
482 drifter survey, we thank Web Pearsall, Brad Hammers, Dan Mulhall, and Steve Robb (NYS
483 Department of Environmental Conservation); Marc Chalupnicki, Sarah Rubenstein, and Gregg
484 Mackey (USGS Tunison Laboratory of Aquatic Science); Suresh Sethi, Mandy Economos, Mike
485 Ashdown, Zena Casteel, and the Shack-Sethi Lab and Limnology Lab groups (Cornell
486 University); and the Keuka Lake Association. Seneca Lake wind data courtesy of John Halfman
487 (Hobart and William Smith Colleges). We thank P.F. and A.J. McCaffrey for their mathematical
488 assistance. Purchase of prototype materials was supported by a Professional Development Grant
489 from Le Moyne College. Additional drifter construction for Keuka Lake was supported by NYS
490 Department of Environmental Conservation, Region 8 Fisheries. Lastly, we thank Tom Manley,
491 Webster Pearsall, Anthony Prestigiacomo, Carl St. John and one anonymous reviewer for their
492 suggestions, which greatly improved this manuscript.

493

494 **Open Research**

495 The dataset used for this research has been deposited on Zenodo and consists of the drifter field
496 deployment, drag experiment, and wind data files. All code using Python version 3.9.13 for
497 statistical analyses is also available on Zenodo via [DOI link here].

498 McCaffrey, L. and Koeberle, A. (2024). Data for An Economical Open-Source Lagrangian
499 Drifter Design to Measure Deep Currents in Lakes. Zenodo. <https://doi.org/#####>.

500 (Note to reviewers, code will be available if considered for publication. Please see code as
501 attached in Supporting Information).

502

503 **References**

- 504 Agade, P., Bean, E. (2023) GatorByte – An Internet of Things-Based Low-Cost, Compact, and
505 Real-Time Water Resource Monitoring Buoy. *HardwareX*, (14), e00427,
506 <https://doi.org/10.1016/j.ohx.2023.e00427>.
- 507 Ahrnsbrak, W. F. 1974. Some additional light shed on surges. *Journal of Geophysical*
508 *Research* **79**: 3482-3483. doi: <https://doi.org/10.1029/JC079i024p03482>
- 509 Austin, J., & Atkinson, S. (2004). The Design and Testing of Small, Low-Cost GPS-Tracked Surface
510 Drifters. *Estuaries*, 27(6), 1026–1029. <http://www.jstor.org/stable/3526977>
- 511 Beng, K. C., and R.T. Corlett. 2020. Applications of environmental DNA (eDNA) in ecology
512 and conservation: opportunities, challenges and prospects. *Biodiversity and*
513 *Conservation* **29**: 2089-2121. doi:<https://doi.org/10.1007/s10531-020-01980-0>
- 514 Bloomfield, J.A. 1978. Lakes of New York State: Ecology of the Finger Lakes, Vol 1. New
515 York: Academic Press, Inc.
- 516 Booth, D.A. On the use of drogues for measuring subsurface ocean currents. *Deutsche*
517 *Hydrographische Zeitschrift* **34**, 284–294 (1981). <https://doi.org/10.1007/BF02226644>
- 518 Bourgault, D., Morsilli, M., Richards, C., Neumeier, U., and Kelley, D.E. 2014 Sediment
519 resuspension and nepheloid layers induced by long internal solitary waves shoaling
520 orthogonally on uniform slopes. *Continental Shelf Research*, 72, 21-33. Doi:
521 <https://doi.org/10.1016/j.csr.2013.10.019>.
- 522 Cadena, A., Vera, S. & Moreira, M. (2018). A low-cost Lagrangian drifter based on open-source
523 hardware and software platform. 4th International Conference on Control, Automation
524 and Robotics, (*ICCAR*), Auckland, New Zealand, pp 218-221.
525 10.1109/ICCAR.2018.8384673.
- 526 Cael, B.B. 2017. The Volume of Earth's Lakes. *Bulletin of the American Physical Society*.
527 <http://meetings.aps.org/link/BAPS.2017.MAR.F12.1>
- 528 Charette, M.A., and W.H.F. Smith. 2010. The volume of Earth’s ocean. *Oceanography* **23**: 112
529 114. doi:<https://doi.org/10.5670/oceanog.2010.51>
- 530 Choi, Jun, Troy, C., Hawley, N., McCormick, M., and M. Wells. 2020. Lateral dispersion of dye
531 and drifters in the center of a very large lake. *Limnology and Oceanography* **65** 336-348.
532 doi: <https://doi.org/10.1002/lno.11302>
- 533 Davis, R. E. 1985. Drifter observations of coastal surface currents during CODE: The method

534 and descriptive view. *Journal of Geophysical Research* **90**: 4741– 4755.
535 doi:10.1029/JC090iC03p04741.

536 Deiner, K. et al. (2017). Environmental DNA metabarcoding: Transforming how we survey
537 animal and plant communities. *Molecular Ecology* **26**: 5872-5895. doi:
538 <https://doi.org/10.1111/mec.14350>

539 Déjeans, B. S., Mullarney, J. C., & MacDonald, I. T. (2022). Lagrangian observations and
540 modeling of turbulence along a tidally influenced river. *Water Resources Research*, 58,
541 e2020WR027894. 4. <https://doi.org/10.1029/2020WR027894>

542 Edwards, K.P., Hare, J.A., Werner, F.E. and B.O. Blanton. 2006. Lagrangian circulation on the
543 Southeast US Continental Shelf: Implications for larval dispersal and retention.
544 *Continental Shelf Research* **26**: 1375-1394. doi:<https://doi.org/10.1016/j.csr.2006.01.020>

545 Feddersen, F., Amador, A., Pick, K., Vizuet, A., Quinn, K., Wolfinger, E., MacMahan J.H., &
546 Fincham, A. (2023) The wavedrifter: a low-cost IMU-based Lagrangian drifter to observe
547 steepening and overturning of surface gravity waves and the transition to turbulence,
548 *Coastal Engineering Journal*, DOI: 10.1080/21664250.2023.2238949

549 Forel, F.A. 1873. Première étude sur les seiches. *Bulletin de la Société Vaudoise des Sciences*
550 *Naturelles* **12**: 213.

551 Foster, G. M., Graham, J. L., Stiles, T. C., Boyer, M. G., King, L. R., and K.A. Loftin. 2017.
552 Spatial variability of harmful algal blooms in Milford Lake, Kansas, July and August
553 2015. No. 2016-5168). U.S. Geological Survey, 2017.
554 doi:<https://doi.org/10.3133/SIR20165168>

555 Fuentes-Pérez, J.F., Sanz-Ronda, F.J. and Tuhtan, J.A. 2022. An Open Surface Drifter for River
556 Flow Field Characterization. *Sensors* 22, no. 24: 9918. <https://doi.org/10.3390/s22249918>

557 Gasser, M., Salvador, J., Sangrà, P., & Pelegrí, J. L. (2001). Field validation of a semi-spherical
558 Lagrangian drifter. *Scientia Marina*, 65(S1), 139–143.
559 <https://doi.org/10.3989/scimar.2001.65s1139>

560 Graham, J. L., Jones, J. R., Jones, S. B., and T. E. Clevenger, T. E. 2006. Spatial and temporal
561 dynamics of microcystin in a Missouri reservoir. *Lake and Reservoir Management*, **22**:
562 59–68. doi:<https://doi.org/10.1080/07438140609353884>

563 Ho, J.C., Michalak, A.M. and N. Pahlevan. 2019. Widespread global increase in intense lake
564 phytoplankton blooms since the 1980s. *Nature*, **574**: 667–670.

565 doi:<https://doi.org/10.1038/s41586-019-1648-7>

566 Hochstaedter, A. and D. Sullivan. 2012. Oceanography and Google Earth: Observing ocean
567 processes with time animations and student-built ocean drifters. *The Geological Society*
568 *of America, Special Paper*, **492**: 441-451. doi:10.1130/2012.2492(34).

569 Hutter, C., & Wang, Y., & Chubarenko, I. (2011). Physics of lakes. Volume 1: Foundation of the
570 Mathematical and Physical Background. Springer-Verlag Berlin-Heidelberg.
571 10.1007/978-3-642-15178-1.

572 Ishikawa, K., Kumagai, M., Vincent, W.F., Tsujimura, S., and H. Nakahara. 2002. Transport and
573 accumulation of bloom-forming cyanobacteria in a large, mid-latitude lake: the gyre
574 *Microcystis* hypothesis. *Limnology*, **3**: 87-96. doi: <https://doi.org/10.1007/s102010200010>

575 Johnson, D., Stocker, R., Head, R., Imberger, J., and C. Pattiaratchi. 2003. A compact low-cost
576 GPS drifter for use in the oceanic nearshore zone, lakes, and estuaries. *Journal of*
577 *Atmospheric and Oceanic Technology*, **20**: 1880-1884. doi: <https://doi.org/10.1175/1520>
578 [0426\(2003\)020<1880:ACLGDF>2.0.CO;2](https://doi.org/10.1175/15200426(2003)020<1880:ACLGDF>2.0.CO;2)

579 Lumpkin, R. and M. Pazos. 2006. Measuring surface currents with Surface Velocity Program
580 drifters: the instrument, its data, and some recent results. Chapter two of Lagrangian
581 Analysis and Prediction of Coastal and Ocean Dynamics (LAPCOD) ed. A. Griffa, A. D.
582 Kirwan, A. J. Mariano, T. Ozgokmen, and T. Rossby.

583 MacDonald, I. T., & Mullarney, J. C. (2015). A novel “FlocDrifter” platform for observing
584 flocculation and turbulence processes in a Lagrangian frame of reference. *Journal of*
585 *Atmospheric and Oceanic Technology*, **32**(3), 547–561. [https://doi.org/10.1175/jtech-d-](https://doi.org/10.1175/jtech-d-14-00106.1)
586 [14-00106.1](https://doi.org/10.1175/jtech-d-14-00106.1)

587 Mackas, D.L., Crawford, W. R., and P. P. Niiler. 1989. A performance comparison for two
588 lagrangian drifter designs. *Atmosphere-Ocean*, **27**: 443-456.
589 doi:10.1080/07055900.1989.9649346

590 Manley, T.O. 2010. Hands-on oceanography: Drifters, drogues, and circulation. *Oceanography*
591 **23**:165–171, doi:10.5670/oceanog.2010.17.

592 Mardani, N., Suara, K., Fairweather, H., Brown, R., McCallum, A., and R.C. Sidle. (2020)
593 Improving the Accuracy of Hydrodynamic Model Predictions Using Lagrangian
594 Calibration. *Water*, **12**:575. <https://doi.org/10.3390/w12020575>

595 McCormick, M.J., Manley, T.O., Beletsky, D., Foley, F.J., and G.L. Fahnenstiel. 2006. Tracking

596 the Surface Flow in Lake Champlain. *Journal of Great Lakes Research*, **34**: 721-730,
597 doi:[https://doi.org/10.1016/S0380-1330\(08\)71613-7](https://doi.org/10.1016/S0380-1330(08)71613-7)

598 McKinney, W. 2010 Data structures for statistical computing in python. Proceedings of the 9th
599 Python in Science Conference, Volume 445, 56-61. Doi: 10.25080/Majora-92bf1922-00a

600 Meyerjürgens, J., Badewien, T. H., Garaba, S. P., Wolff, J. O., and O. Zielinski. 2019. A state
601 of-the-art compact surface drifter reveals pathways of floating marine litter in the German
602 bight. *Frontiers in Marine Science*, **6**: 58. doi: <https://doi.org/10.3389/fmars.2019.00058>

603 Mullarney, J.C. and Henderson, S.M. (2013) A novel drifter designed for use with a mounted
604 Acoustic Doppler Current Profiler in shallow environments. *Limnol. Oceanogr.: Methods*,
605 **11**, 438-449. Doi: <https://doi.org/10.1175/JTECH-D-14-00106.1>

606 Mullins, H.T., Hinchey, E.J., Wellner, R.W., Stephens, D.B., Anderson, W.T., Dwyer, T.R. and
607 A.C. Hine. 1996. Seismic stratigraphy of the Finger Lakes: a continental record of
608 Heinrich event H-1 and Laurentide ice sheet instability. *Geological Society of America*
609 *Special Paper* 311, pp.1-36

610 Nakayama, Y. 2018. Introduction to Fluid Mechanics (Second Edition), Butterworth-Heinemann,
611 ISBN 9780081024379, <https://doi.org/10.1016/B978-0-08-102437-9.00009-7>.

612 Novelli, G., Guigand, C.M., Cousin, C., Ryan, E.H., Laxague, N.J.M., Dai, H., Haus, B.K. and
613 Özgökmen, T.M. 2017. A biodegradable surface drifter for ocean sampling on a massive
614 scale. *J Atmos Ocean Tech.* 34(11):2509-32. <http://doi.org/10.1175/JTECH-D-17-0055.1>.

615 Niiler, P.P., Sybrandy, A.S., Bi, K., Poulain, P.M., and Bitterman, D. (1995). Measurements of
616 the water-following capability of holey-sock and TRISTAR drifters. *Deep Sea Research*
617 *Part I: Oceanographic Research Papers*, **42**: 1951-1964. doi:
618 [https://doi.org/10.1016/0967-0637\(95\)00076-3](https://doi.org/10.1016/0967-0637(95)00076-3).

619 Pauli, V. et al., and SciPy 1.0 Contributors. (2020) SciPy 1.0: Fundamental Algorithms for
620 Scientific Computing in Python. *Nature Methods*, **17**(3), 261-272.

621 Postacchini, M., Centurioni, L. R., Braasch, L., Brocchini, M., & Vicinanza,
622 D. (2015). Lagrangian observations of waves and currents from the river drifter. *IEEE*
623 *Journal of Oceanic Engineering*, **41**(1), 94–104.

624 Poulain P-M, Centurioni L, Özgökmen T. (2022) Comparing the Currents Measured by
625 CARTHE, CODE and SVP Drifters as a Function of Wind and Wave Conditions in the
626 Southwestern Mediterranean Sea. *Sensors*. **22**(1):353. <https://doi.org/10.3390/s22010353>

627 Pacific Gyre. 2023.

628 [https://www.pacificgyre.com/support/carthe/Content/products/carthe/CARTHE%20Speci](https://www.pacificgyre.com/support/carthe/Content/products/carthe/CARTHE%20Specifications.htm)

629 [fications.htm](https://www.pacificgyre.com/support/carthe/Content/products/carthe/CARTHE%20Specifications.htm), retrieved on 22 March 2023.

630 Sabet, B. S., & Barani, G. A. (2011). Design of small GPS drifters for current measurements in

631 the coastal zone. *Ocean & Coastal Management*, **54**(2), 158–

632 163. <https://doi.org/10.1016/j.ocecoaman.2010.10>.

633 Spencer, D., Lemckert, C.J., Yu, Y., Gustafson, J., Lee, S.Y., Zhang, H., 2014. Quantifying

634 Dispersion in an Estuary: A Lagrangian Drifter Approach. In: Green, A.N. and Cooper,

635 J.A.G. (eds.), Proceedings 13th International Coastal Symposium (Durban, South Africa),

636 Journal of Coastal Research, Special Issue No. 70, pp. 029-034, ISSN 0749-0208.

637 Sakai, Y., Murase, J., Sugimoto, A., Okubo, K. and E. Nakayama. 2002. Resuspension of bottom

638 sediment by an internal wave in Lake Biwa. *Lakes & Reservoirs: Research &*

639 *Management*. **7**: 339 - 344. doi:10.1046/j.1440-1770.2002.00200.x.

640 Stocker, R., and J. Imberger. 2003: Horizontal transport and dispersion in the surface layer of a

641 medium size lake. *Limnol. Oceanogr.*, **48**, 971–982. doi:

642 <https://doi.org/10.4319/lo.2003.48.3.0971>

643 Suara, K. A., Wang, H., Chanson, H., Gibbes, B., & Brown, R. J. (2018). Response of GPS-

644 tracked drifters to wind and water currents in a tidal estuary. *IEEE Journal of Oceanic*

645 *Engineering*, **44**(4), 1077–1089.

646 Subbaraya, S., Breitenmoser, A., Molchanov, A., Muller, J., Oberg, C., Caron, D.A. and

647 Sukhatme, G.S. (2016). Circling the Seas: Design of Lagrangian Drifters for Ocean

648 Monitoring. *IEEE Robotics & Automation Magazine*, **23**: 42-53.

649 doi:10.1109/MRA.2016.2535154

650 Sybrandy, A. L. and P. P. Niiler. 1992. WOCE/TOGA Lagrangian drifter construction manual.

651 WOCE Rep. 63, SIO Ref. 91/6. Scripps Inst. of Oceanogr., 58 pp.

652 van Brummelen, G.R. 2013. Heavenly Mathematics: The Forgotten Art of Spherical

653 Trigonometry. Princeton University Press. ISBN 9780691148922.

654 Wetzel, R.G. 2001. Limnology: Lake and River Ecosystems. Academic Press, San Diego,

655 pp1024. ISBN: 9780127447605

656 Wynne, T. T., et al. 2013. Evolution of a cyanobacterial bloom forecast system in western Lake

657 Erie: Development and initial evaluation. *Journal of Great Lakes Research*, **39**: 90-99.

